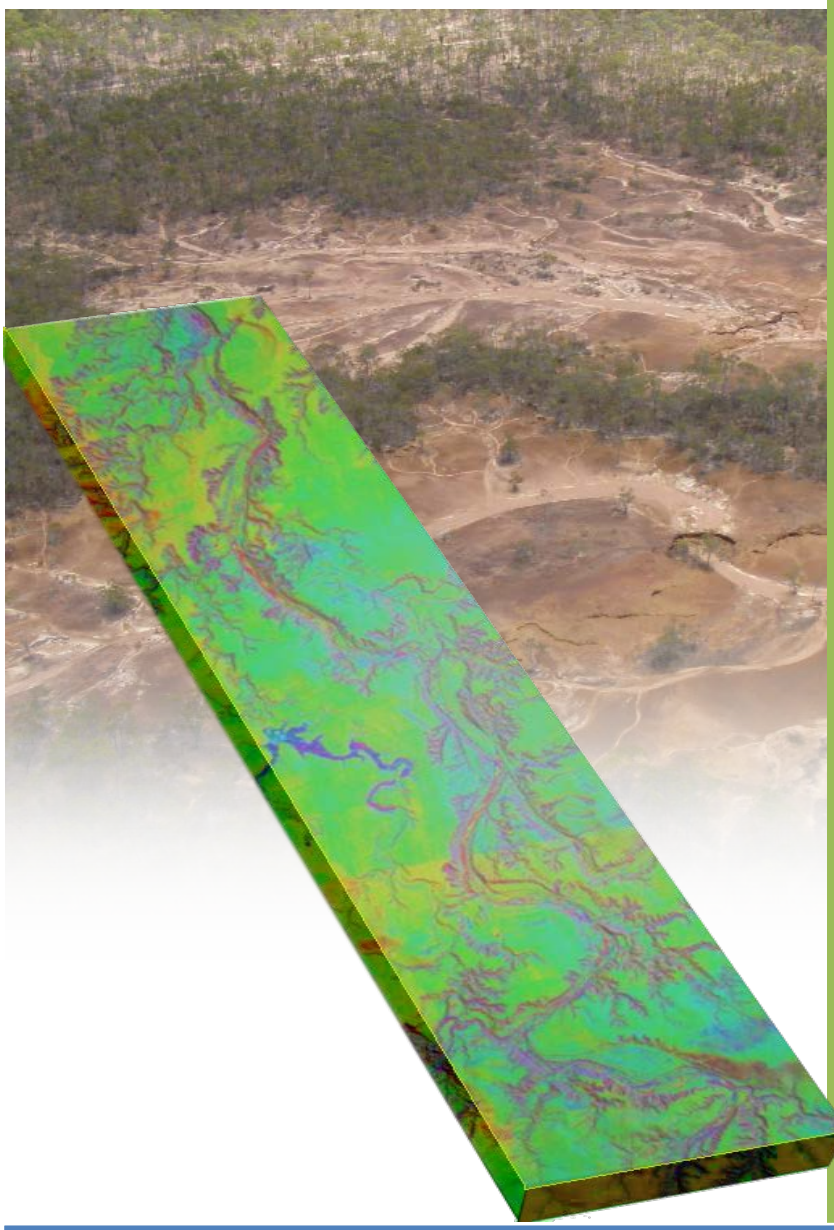

An Empirically-based Sediment Budget for the Normanby Basin

Andrew Brooks, John Spencer, Jon Olley, Tim Pietsch, Daniel Borombovits, Graeme Curwen, Jeff Shellberg, Christina Howley, Angela Gleeson, Andrew Simon, Natasha Bankhead, Danny Klimetz, Leila Eslami-Endargoli, Anne Bourgeault

Australian Rivers Institute

Griffith University

Appendix 04: Air photo Change Detection Methods – Medium term Sediment Production

Griffith UNIVERSITY

CARING FOR OUR COUNTRY

Appendix to the Final Report prepared for the Australian Government's Caring for our Country - **Reef Rescue initiative**

IMPORTANT

This document is current at the date noted. Due to the nature of collaborative academic publishing, this content is subject to change and revision. Please see the Cape York Water Quality website for more info:

http://www.capeyorkwaterquality.info

This Version: 3/03/2013

CAPE YORK WATER QUALITY

Appendix 04: Air photo Change Detection Methods – Medium term Sediment Production

Prepared by: Graeme Curwen and Andrew Brooks

1 Rationale

Historic air photo analysis has been used elsewhere to determine multi-decadal trends in the rate of alluvial gully expansions (Shellberg, 2011a; Shellberg et al., 2010; Shellberg et al., 2013 forthcoming). An air photo image provides a snapshot in time of landscape condition, allowing the location, size and distribution of gullies and other features to be mapped back as far as the early 1950s.

By georeferencing the air photo to the recent LiDAR data, changes in gully area through time can be made, and by reconstruction of the land surface that that has subsequently eroded, it is possible to estimate the change in gully volume through time, and hence that actual erosion rate.

By looking at a time series of photos over multiple decades, it is then possible to reconstruct erosion rates through time. By then developing a dimensionless relationship between area and time, it is then possible to establish via linear regression the approximate time of initiation of individual gullies *sensu* (Shellberg, 2011a).

The calculated medium term rate of erosion can be compared to the rate of erosion calculated over the much shorter interval (2 years) derived from repeat LiDAR.

2 Historical Air Photo data set

The Queensland Department of Environment and Resources (DERM) maintains a library of approximately 2 million aerial photos of all parts of Queensland, dating back to the 1930's (The Queensland Air Photo (QAP) series). The air photo index identified 7596 images in the Normanby catchment, spanning from 1937 to 2006, with several hundred falling within the extent of the 50 LiDAR Blocks, that were the focus of this analysis. The process of rectifying the images was much more feasible with the LiDAR as a base data set to work with. The series of high resolution (15μm) scans of the photo negatives were acquired with the generous assistance of Terry Culpitt, Ron deBoer, Mike Ruckert, and Peter Manson in the Imagery Coordination Program at the Queensland Department of Environment and Resource Management (QDERM).

3 Air photo metadata for QAP photos.

Table 1 Information listed for each air photo in the QAP series

IDCODE	FOCALLENGT (152.23 – 153.2mm)	LAT
TITLE	RUNINFORID	LONG
SCALE (12000 to 84700)	RUN	ZONE
KEYDIAGRAM	FILMPREFIX	EASTING
STORAGE	FILM	NORTHING
FLYING (date)	CDPREFIX	MAPNO
NEGATIVE (bw or colour)	CDNO	IMAGEID
FLYINGHEIG (12750ft to 7620m)	CDBYAREA	FORMAT
DATUMHEIGH (0ft to 800m)	FRAME	RESOLUTION

Original air photo negatives were scanned at 1693 dpi and delivered in tiff format (http://www.derm.qld.gov.au/property/mapping/aerial_photography.html)

4 Air photo selection

The centre of each QAP air photo was represented by a point in a shapefile. All QAP points within a buffer of 1km were acquired from DERM. Air photos for each block were evaluated from the most recent to the oldest, with the aim of establishing the most detailed time series possible from the available photos, within which there were visible gullies, at a scale that could be mapped with a reasonable degree of accuracy. Where several photos for a given year were available, preference would be given to photos with their centre closest to the centre of the LiDAR block, and with the visible gully closest to the centre of the photo. Working with the central part of the photo meant there was less distortion, making it easier to rectify the photos.

Table 2 Air photos used in the time series analysis to determine multi-decadal rates of gully erosion (see Appendix X for the metadata on the individual photo runs for each time slice). This is a subset of a larger dataset used to establish long term rates, however, data from 7 of the blocks were discarded due to QA concerns with the LiDAR data.

LiDAR Block	Number of air photo gullies	Number of gullies covered by repeat LiDAR	Year of air photo			
n04	1	1	1952	1957	1987	1994
n05	4	4	1952	1957	1982	1987
n09	2	2	1951	1987	1994	
n10	1	1	1952	1986		
n13	2	0	1951	1984		
n14	2	1	1952			

n16	1	1	1952	1987		
n17	2	2	1952	1987		
n18	1	0	1952	1987		
n20	1	1	1951	1987		
n21	3	0	1951	1987		
n23	1	0	1951	1987		

5 Distortions to air photos and Georeferencing

Several kinds of distortion and displacement affect the apparent location of features in historical air photos (Thomas Lillesand, 2008). These include, but are not limited to:

- Distortions in the scanning process of negatives to digital format
- Relief displacement of objects in hilly country
- Roll, pitch and yaw of the plane
- Characteristics of the lens system

It was found that an air photo could not be georeferenced once and get all features in the air photo to align with all features in the LiDAR image. Hence, each gully of interest had an air photo georeferenced specifically for that gully, using features as close to the gully as possible, with 4 control points to test Total Root Mean Square Error (TRMSE). A TRMSE value under 2 was deemed acceptable, which means modelled location of georeferenced points were within 2 m of actual location (WinTopo, 2010).

Georeferencing air photos in remote savannah landscapes with few permanent features and very few persistent built structures can be extremely challenging. Preferred features for georeferencing air photos were consistently identifiable between photos, and were stark and immobile in the landscape, such as rocks, water tanks, buildings and isolated trees. Features likely to be moved by human action were used with caution, such as road intersections, fences, bridges. If other options were scarce, stable natural features in the landscape were used, such as stable channels and ridges.

6 Digitising gully outlines

Once georeferenced, the outline of a gully head scarp was digitised, with cross referencing to LiDAR imagery to ensure reflective bare ground outside the gully was not mistakenly included as gully area. Contrast enhancing stretches were used to assist headwall identification. The initiation point or starting area of a gully was located at: a) the confluence of that gully outflow with an adjacent gully outflow; b) the confluence of the narrow gully neck with a vegetated meandering secondary channel; c) the transition from confined gully walls to main channel floodplain or riverbed.

Metrics calculated for each historical gully at each time slice were: 1) area; 2) perimeter; 3) difference in area between historical extent and 2009 LiDAR derived extent; 4) linear length

from gully starting point to furthest headwall; 5) volume of the area beneath the "zone of difference" from the historical extent and the 2009 outline, calculated from a reconstructed surface and the 2009 DEM (see below 7)

7 Reconstructed surfaces

A reconstructed surface modelling the flood plain prior to gully inception was built for each for each air photo gully. Values for interpolating the reconstructed surface were obtained by buffering 2009 gully perimeter by 5m, converting the buffered line to points with 1m spacing and extracting values beneath each point from the 2009 DEM to a new point shapefile. Points were manually added to obtain heights of non-eroded pedestals or ridges with in a gully. Points across the gully exit were assigned values of the floodplain on either side of the gully mouth. The reconstructed surface was generated using ArcMap 10 IDW interpolator, with a cell size of 1m that was aligned to DEM cells using snap raster.

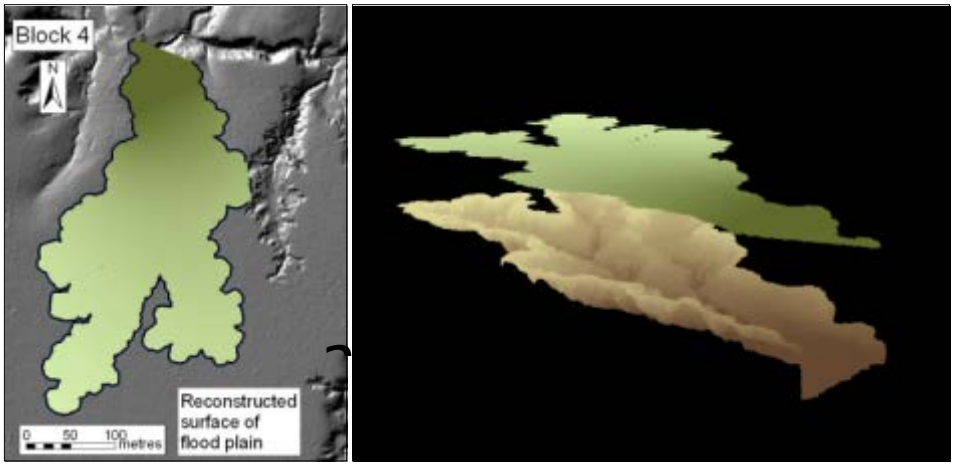

Figure 1 Reconstructed flood plain surface of air photo gully 1 in Normanby 4 in a) plan view and b) with vertical offset to see underlying gully detail

8 Calculating erosion rates from air photo gullies

With the position of gully perimeter fixed for two time intervals, e.g. 1952 and 2009 (figure 3.2 a) the area between the digitised lines represented expansion of the gully between the two dates. Volume of erosion was calculated using the zonal statistics tool in the Spatial Analyst tool box of Arc Map 10; within the zone of difference (Figure 2 b – orange area) the sum of elevations of the DEM was subtracted from the sum of values for the reconstructed surface, the product being volume in m^3.

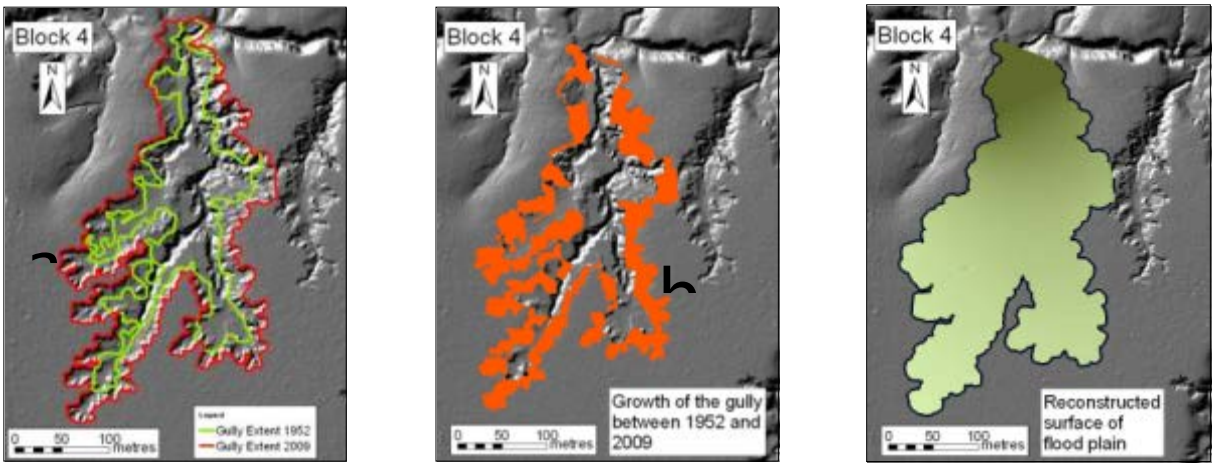

Figure 2 a) Historical and recent gully extent from 1952 air photo and 2009 LiDAR imagery. b) The zone of difference, representing erosion between 1952 and 2009

9 Assumptions and limitations of historical erosion rates

The interpolation of a change in gully area into a change in gully volume includes some inherent error, which causes the calculated volumetric change to under estimate the true extent of change. We can measure the horizontal distance between gully perimeters at the two times (Figure 3), but the extent of down cutting of the gully floor between air photo date and LiDAR date is not known.

Our analysis assumes that the gully floor at time 1 is the same as at time 2, and that all of the change is represented by headwall expansion. We know however that this is not the case (Shellberg, 2011a), and so the volumetric change estimates derived using this method could be underestimating the true erosion rate by a factor of 1 – 2. Indeed, in the example shown in it is evident that there is a major new incisional episode working its ways through the gully, which will not have been captured by the air photo analysis.

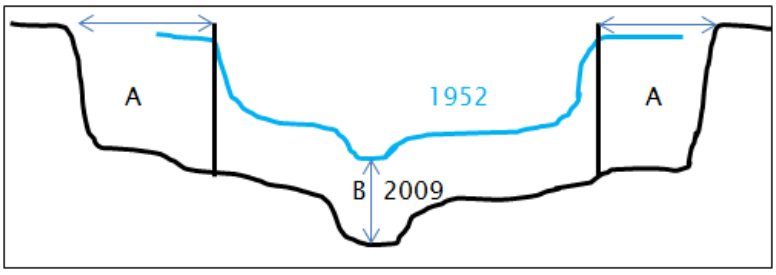

Figure 3 Longitudinal diagram of difference in horizontal (A) and vertical (B) position of an air photo gully and recent gully profile from LiDAR. Not to scale.

The zone of difference modelled in Figure 3 had vertical walls, the same as modeled in the GIS, which in reality would have been sloping to some degree. This would lead to an overestimation of the volume of change.

The area B represents a volume of erosion that is not captured with this modelling, and the volume of real erosion is underrepresented by the volume that exists between the gully floor in 1952 and 2009. This underestimation will have vastly outweighed any type a) error.

Hence for the reasons outlined here, the long term erosion rates calculated from the air photo analysis are extremely conservative, particularly as secondary incision of gully floors seems to be a widespread phenomenon in many of the gullies we have observed throughout the Normanby Catchment.

10 Historical Air Photo Gully Results

The outline of twenty one gullies in 13 LiDAR blocks were digitised from air photos and also from LiDAR flown in 2009. Nine of the air photo gullies were also digitised from orthophotos collected at the time of flying 2009 LiDAR. The greatest number of air photo time slices per block was 4, the least 1, with the average being 2.1. Even with only one historical area estimate a long term rate can be calculated, when compared with the most recent LiDAR data. Three blocks had imagery covering 60 years, from 1951 to (LiDAR in) 2011, eight blocks had imagery from 1952 to 2011. Every air photo gully had area calculated from LiDAR flown in 2009, but only 13 of 21 gullies covered by repeat LiDAR, had erosion volumes calculated.

Table 3: Dates of air photos

Date of Imagery	Number of images
1951	9
1952	10
1982	1
1984	2
1987	15
1994	3
Total Number of Images	40

Table 4: List of 21 gullies digitised from air photos. Only gullies covered by repeat LiDAR were able to have erosion rates calculated based on historical air photo area.

Gully code	Area in 2009 ha	Repeat or no repeat LiDAR		Gully	Area in 2009 ha	Repeat or no repeat LiDAR
N04 g1	4.7	repeat		N16 g1	2.8	repeat
N05 eg1	0.33	repeat		N17 g1	1.06	repeat
N05 eg2	0.3	repeat		N17 g2	1.78	repeat
N05 eg3	1.81	repeat		N18 g1	1.73	no
N05 wg1	4.08	repeat		N20 g1	6.32	repeat
N09 g1	1.21	repeat		N21 g1	2.47	no

N09 g2	1.33	repeat		N21 g2	3.33	no
N10 g1	2.54	repeat		N21 g3	0.37	no
N13 g1	1.09	no		N23 g1	0.99	no
N13 g2	4.5	no				
N14 g1	5.97	no				
N14 g3	53.85	repeat				

11 Erosion rates from air photo and LiDAR imagery.

Table 5: Dates of air photo imagery, gully area at that time, area of gully expansion between air photo date and 2009, and calculations of erosion volume for 13 gullies covered by repeat LiDAR.

Gully code	Image date	Interval to 2009 yr	gully area from image ha	Perimeter m	Difference in area between date of image and 2009 ha	Volume of erosion from date of image to 2009 m3	Rate of erosion per year m3/yr	Rate of erosion per area of gully expansion m3/ha/yr	Volume of erosion normalised to 2009 gully area m3/ha/yr
N04 g1	1952	57	2.18	2065	2.43	26816	470	193	100
N04 g1	1957	52	2.63	1607	2.14	23243	447	208	95
N04 g1	1987	22	3.19	2061	1.47	9723	442	300	94
N04 g1	1994	15	3.50	2278	1.11	8916	594	536	127
N04 g1	2009	0	4.70	2570					
N04 g1	2011	2	4.70	2570	0.03	183	92	3050	19
N05 eg1	1987	22	0.19	232	0.26	160	7	28	22
N05 eg1	2009	0	0.33	304					
N05 eg1	2011	2	0.33	304	0.00	18	9	3114	28
N05 eg2	1952	57	0.12	286	0.32	854	15	46	51
N05 eg2	1987	24	0.20	340	0.25	648	27	109	91
N05 eg2	2009	0	0.30	373					
N05 eg2	2011	2	0.30	373	0.00	0	0	0	0
N05 eg3	1952	57	1.57	794	0.24	4789	84	353	47
N05 eg3	1957	52	1.33	697	0.47	11555	222	468	123
N05 eg3	1982	27	1.58	858	0.23	5514	204	906	113
N05 eg3	1987	22	1.51	807	0.29	8333	379	1304	210
N05 eg3	2009	0	1.81	830					
N05 eg3	2011	2	1.81	834	0.02	167	84	3669	46
N05 wg1	1952	57	2.88	3426	1.46	25905	454	311	111

N05 wg1	1987	24	3.47	2748	0.79	9453	394	499	97
N05 wg1	2009	0	4.08	3210					
N05 wg1	2011	2	4.37	3289	0.02	108	54	3014	13
N09 g1	1951	58	0.69	450	0.52	6071	105	200	86
N09 g1	1987	22	0.74	731	0.47	4365	198	418	164
N09 g1	1994	15	0.79	520	0.42	4833	322	764	266
N09 g1	2009	0	1.21	628					
N09 g1	2011	2	1.21	630	0.01	90	45	3443	37
N09 g2	1951	58	0.62	916	0.70	13618	235	334	177
N09 g2	1987	22	1.09	794	0.24	2612	119	493	89
N09 g2	1994	15	1.05	699	0.28	4802	320	1155	241
N09 g2	2009	0	1.33	1116					
N09 g2	2011	2	1.33	1128	0.05	423	212	4514	160
N10 g1	1952	57	2.07	1090	0.47	11643	204	435	81
N10 g1	1986	23	2.10	1219	0.45	9912	431	968	170
N10 g1	2009	0	2.54	1246					
N10 g1	2011	2	2.54	1280	0.06	530	265	4413	104
N14 g3	1952	57	21.88	22000	31.45	218562	3834	122	71
N14 g3	2009	0	53.85	32618					
N14 g3	2011	2	53.97	36291	1.63	8347	4174	2560	77
N16 g1	1952	57	1.78	1228	1.01	11913	209	206	75
N16 g1	1987	22	1.86	1377	0.93	9854	448	481	160
N16 g1	2009	0	2.80	1180					
N16 g1	2011	2	2.80	1187	0.00	84	42	86200	15
N17 g1	1952	57	0.37	590	0.69	10564	185	268	175
N17 g1	1987	22	0.72	909	0.33	2805	127	381	121
N17 g1	2009	0	1.06	965					
N17 g1	2011	2	1.06	998	0.03	1209	604	21737	571
N17 g2	1987	22	1.39	1048	0.40	2780	126	319	71
N17 g2	2009		1.78	1206					
N17 g2	2011	2	1.79	1195	0.01	32	16	2439	9
N20 g1	1951	58	4.89	2407	1.46	10380	179	123	28
N20 g1	1987	22	5.24	2258	1.13	7328	333	295	53
N20 g1	2009	0	6.32	2392					571
N20 g1	2011	2	6.32	2397	0.01	35	18	2347	3

12 Variation in rate of erosion based on 5 decade air photo record

The volume of material eroded from gullies was normalized by dividing the volume of erosion by the number of years in the time period, giving a measure of which gullies were moving larger or smaller amounts in total per annum. Using this calculation, the minimum volume eroded was 15m^3/yr (N5 eg2), maximum 3834m^3/ha (N4 g3), average 511m^3/yr (s.d. 214m^3/yr excluding outliers).

Another approach used was to normalise volume of erosion per year to the increase in gully area between the date of air photo and 2009 LiDAR capture. Data from 11 gullies covered by 1951 and 1952 air photos showed a minimum annual erosion loss of 46m^3/ha of gully expansion, maximum loss of 435m^3/ha of gully expansion, and an average rate of 236m^3/ha (s.d. 110). Larger losses per hectare indicate a greater depth of erosion.

A third approach to quantifying rate of erosion, and possibly the most useful for up-scaling rate of erosion from air photo gullies, was to normalise annual volume of material eroded since the early 1950s to the gully area in 2009. Minimum rate from 11 gullies was 28m^3/ha/yr, maximum 325m^3ha/yr, and average 91m^3/ha/yr (s.d. 46). This rate was used in the extrapolation of unit area rates to the broader gully area dataset at the catchment scale.

13 Variation in rates of erosion from air photo and LiDAR analysis

Air photos from different decades covering the same gullies allowed comparison of rates of erosion over a decadal scale (table 3). Repeat LiDAR coverage with a 2 year interval allowed calculation of contemporary erosion rates. For 13 gullies, the minimum and average rates of erosion over 5 decades between the 1950s and 2009 was a similar order of magnitude to the rate over 20 years from the 1980s to 2009. Maximum rate of erosion from the 1950s to 2009 was 14% of the rate from the 1980s to 2009. Whether this represents a true slow down in erosion rates or a data processing issue has yet to be determined. However, it is possible that it is the later, as the photo resolution was poor for the period through the 1980s and 90s

Rates of erosion calculated from repeat LiDAR for 13 gullies ranged from minimum 0 m^3/ha/yr to maximum 571 m3/ha/yr. Average rate of erosion calculated from repeat LiDAR was 115 m^3/ha/yr, 26% above the average rate over 60 years calculated from air photo analysis.

This suggests intense erosion activity over the 80s and 90s, far in excess of the average over 3 decades prior to the 1980s. The climate record has not been checked to correlate erosion rates with rainfall, but this could provide an explanation or establish a correlation with rainfall as a driver of rates of erosion in this study area.

Table 6: Rates of erosion based on 50 and 20 year air photo record, and 2 year interval for repeat LiDAR.

	Yield: volume material lost divided by area of 2009 gully divided by interval m3/ha/yr		
	Air photo data		LiDAR data
	1950s to 2009	1980s to 2009	2009 to 2011
N04 g1	100	94	470
N05 eg1	no data	22	28
N05 eg2	51	91	0
N05 eg3	47	161	46
N05 wg1	111	97	13
N09 g1	86	164	37
N09 g2	177	89	160
N10 g1	81	170	104
N14 g3	71	no data	77
N16 g1	75	160	15
N17 g1	175	121	571
N17 g2	no data	71	9
N20 g1	28	53	3
min	28	22	0
max	177	210	571
average	91	112	115

14 Predicting gully age from area increase

Ten gullies with a minimum 4 area measurements (Figure 4) at different dates were used in a linear regression to predict initiation dates of gullies. The base year was the first year a gully was digitised (A), and subsequent images were Ao. Thus first gully area would always be zero, and larger areas would be greater than one, except in cases where gullies showed recovery.

Gullies with less than 4 area measurements were not included in this analysis. R^2 values ranged from 0.61 to 0.99. Predicted initiation date of 5 gullies fell between 1880 and 1930; one gully at approximately 1860 and 4 gullies earlier than 1850 by decades or hundreds of

years. These patterns are consistent with those found in adjacent the Mitchell catchment, (Shellberg, 2011b), although the phase of recent predicted gully initiation in the Mitchell was later than for the Normanby, during the 1930s and 1940s, an offset of approximately 30 years. It is interesting to note that cattle were introduced to the Normanby (Howley, 2005) and Mitchell (Shellberg et al., 2009) catchments during the 1870s and 1880s, in response to demands of gold diggers.

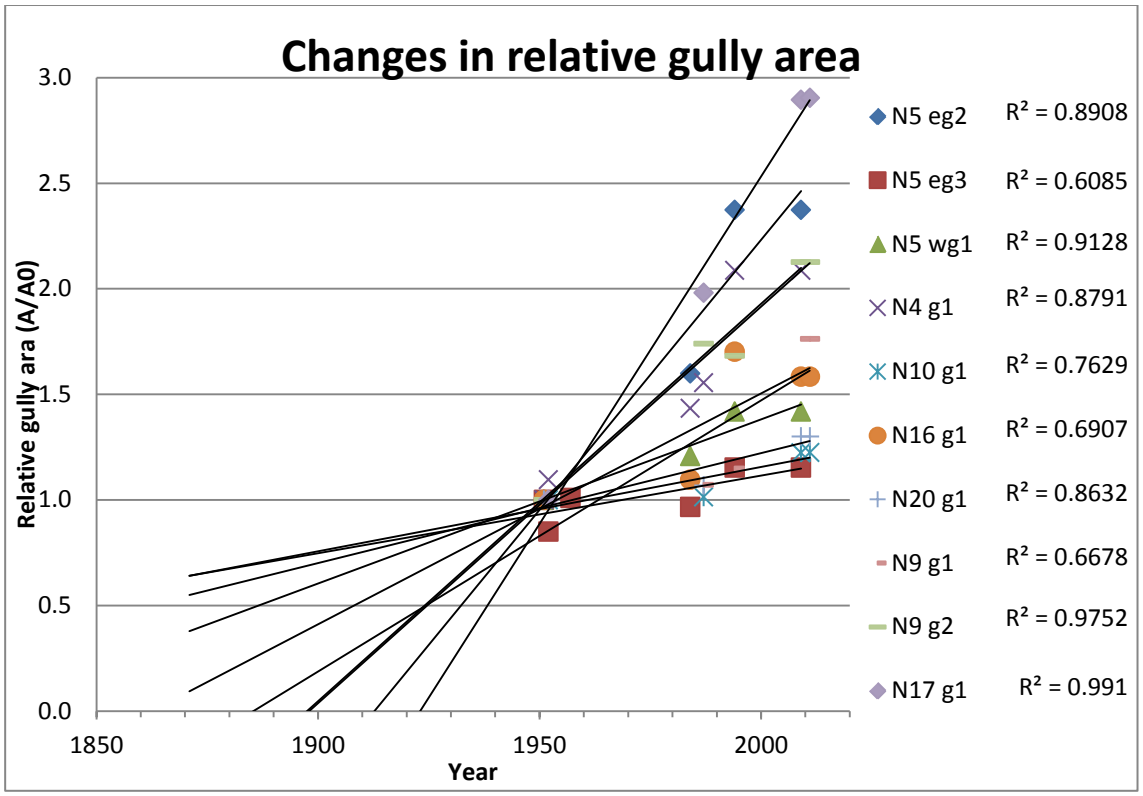

Figure 4 Change in relative gully area for 10 selected gullies with a minimum of 4 area measurement each.

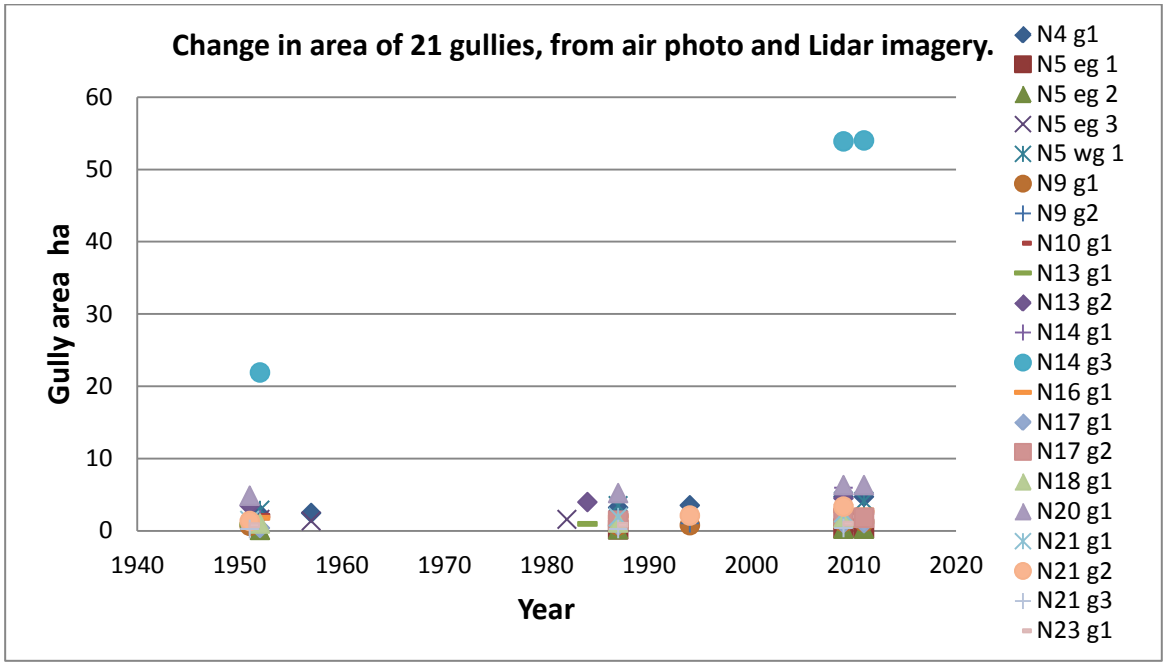

Figure 5 Raw gully area from air photo and LiDAR imagery, all 21 gullies on the same graph

Trend lines have not been fitted to Figure 5 as it would become very busy down the bottom of the graph.

Error bars have not been fitted, but a 10% error has been assumed to account for human error and differences between air photos by(Lawler, 1993), cited by (Saxton et al., 2012). Sources of error to accurately defining gully perimeter from air photos include: RMSE (Root Mean Squared Error) from georeferencing air photos – average RMSE from 40 images was 1.71, spacing vertices around gully perimeter, map scale during digitising, presence of vegetation obscuring gully wall, bare ground beyond gully indistinguishable from gully surface, other human factors.

The obvious outlier, N14 g3 was 21.8ha in 1952 and 53.8 ha in 2011. A linear gully 4.3km in length, had rapid expansion of head scarps on multiple fronts by 2011, little lateral expansion along the length of the gully, and appears to be being driven by overland flows from the main Normanby channel approximately 4 km distant. LiDAR imagery shows pitting and pugging along the flow path between the main channel and the head of the gully, suggesting rapid transformation to a channel will occur.

Minimum area of an air photo gully at the first time slice was 0.12ha (N5 eg2, 1952), maximum area was 21.88ha (N14 g3, 1952), and average area, excluding N14 g3 outlier was 2.44ha.

By 2009, the smallest gully, N5 eg2 had expanded by 0.18ha to 0.3ha, and the largest gully, N14 g3, had expanded to 53.97ha. Average area of gullies, as measured from 2009 LiDAR, excluding N14g3 outlier, was 2.43ha.

An increase in area was measured for all air photo gullies, with the minimum area increase 0.11ha (N13 g1, 1987 to 2009), maximum increase 31.5ha (N14 g3, 1952 to 2009), and average increase 2.99ha.

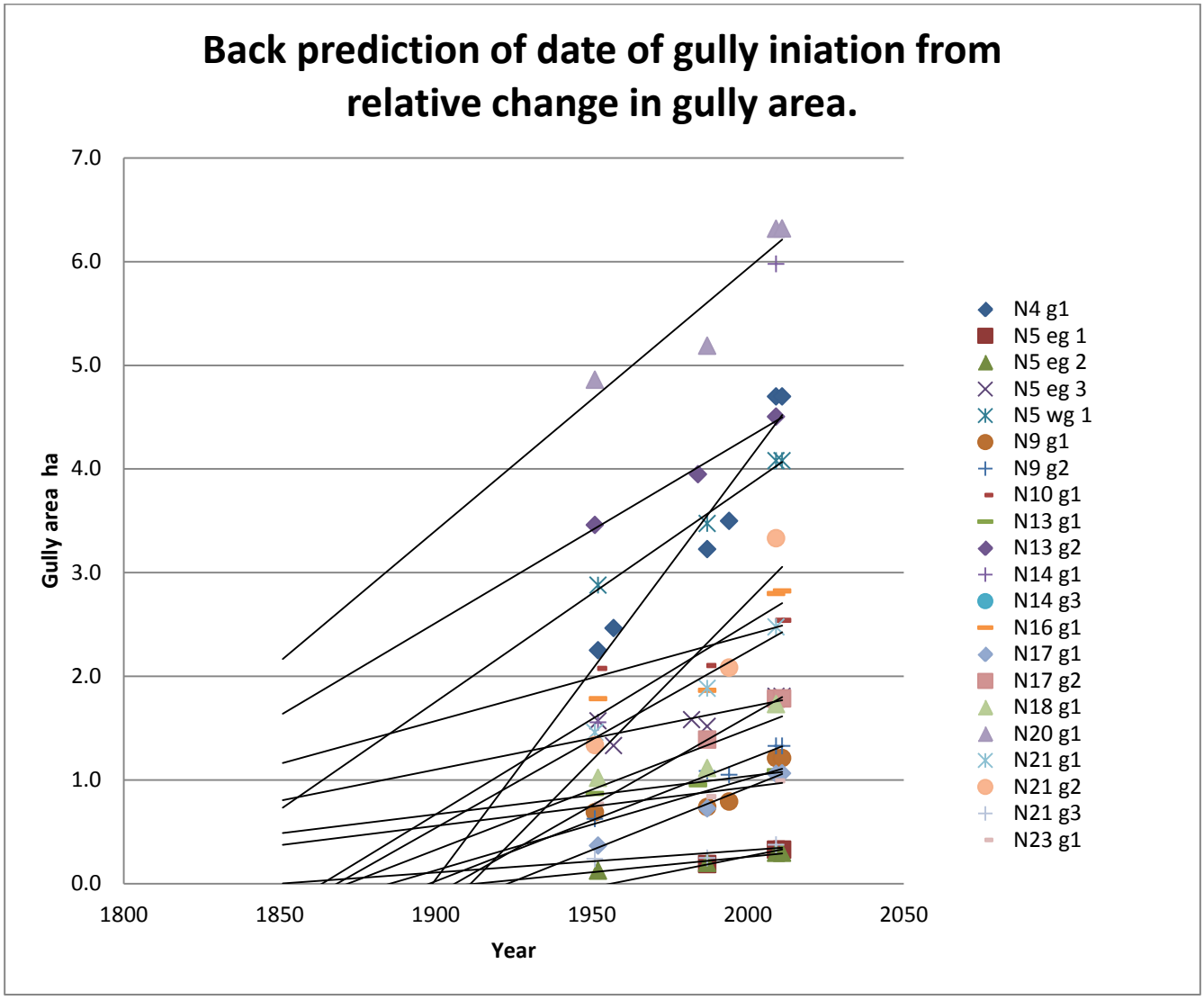

Figure 6: Change in relative gully area of 21 gullies. Each gully was covered by repeat LiDAR. Two phases of initiation are suggested by this data. A phase between 1850 and 1950, and a phase prior to 1800 that cannot be accurately predicted due to limitations of the data set. This graph has the same data as Figure 4 above, but with outliers removed. Figure 4 above has the 10 best time series presented. 11 of the data series in fig 3 have 3 or less points, which I thought was getting too few to use for back predicting gully initiation from.

15 References

See also main report: http://www.capeyorkwaterquality.info

Howley, C.a.S., K., 2005. LAURA-NORMANBY CATCHMENT MANAGEMENT STRATEGY, Environmental Consultants.

Lawler, D.M., 1993. The measurement of river bank erosion and lateral channel change: A review. Earth Surface Processes and Landforms, 18(9), 777-821.

Saxton, N.E., Olley, J.M., Smith, S., Ward, D.P., Rose, C.W., 2012. Gully erosion in sub-tropical south-east Queensland, Australia. Geomorphology, 173-174(0), 80-87.

Shellberg, J., Brooks, A., Spencer, J., Knight, J., 2009. Alluvial gully erosion rates across the Mitchell River fluvial megafan, Queensland, Australia, 7th International Conference on Geomorphology (ANZIAG), Melbourne.

Shellberg, J.G., 2011a. Alluvial Gully Erosion Rates and Processes Across the Mitchell River Fluvial Megafan in Northern Queensland, Australia. PhD Dissertation, Griffith University, Australian Rivers Institute, School of Environment.

Shellberg, J.G., 2011b. Alluvial Gully Erosion Rates and Processes Across the Mitchell River Fluvial Megafan in Northern Queensland, Australia. Griffith University, Brisbane, Australia, pp. PhD Thesis.

Shellberg, J.G., Brooks, A.P., Spencer, J., Knight, J., Pietsch, T., 2010. Rates of alluvial gully erosion across the Mitchell River fluvial megafan, Queensland, Australia. In: W. Zglobicki (Ed.), Human Impact of Gully Erosion, 5th International Symposium on Gully Erosion, Book of Abstracts. Maria-Curie Sklodowska University, Institue of Earth Sciences, Lublin, Poland, April 19-24, 2010, pp. 109.

Shellberg, J.G., Spencer, J., Brooks, A.P., Pietsch, T., 2013 forthcoming. Alluvial gully erosion rates across the Mitchell River fluvial megafan, northern Australia. Target Submission: Geological Society of America Bulletin.

Thomas Lillesand, R.W.K., Chipman Jonathon W 2008. Remote Sensing and Image Interpretation. Wiley and Sons, USA.

WinTopo, 2010. WinTopo Raster to Vector Converter, SoftSoft Ltd, 12a Hitchin St., Biggleswade, Bedfordshire, SG18 8AX, UK, pp. WinTopo is a high quality software application for converting TIF, JPG, PNG, GIF, BMP files and scanned images into useful vector files suitable for CAD, GIS and CNC applications.